ACADEMIC PRESS

Journal of Solid State Chemistry 169 (2002) 118–124

JOURNAL OF SOLID STATE CHEMISTRY

www.academicpress.com

Complex three-dimensional platinum–indium networks in the ternary indides $Dy_2Pt_7In_{16}$ and $Tb_6Pt_{12}In_{23}$

Vasyl' I. Zaremba,[a,b] Yaroslav M. Kalychak,[a] Vitaliy P. Dubenskiy,[a] Rolf-Dieter Hoffmann,[b] Ute Ch. Rodewald,[b] and Rainer Pöttgen[b,*]

[a] *Inorganic Chemistry Department, Ivan Franko National University of Lviv, Kyryla and Mephodiya Street 6, 79005 Lviv, Ukraine*
[b] *Institut für Anorganische und Analytische Chemie, Universität Münster, Wilhelm-Klemm-Straße 8, D-48149 Münster, Germany*

Received 12 June 2002; received in revised form 16 August 2002; accepted 25 August 2002

Abstract

Well crystallized samples of $Dy_2Pt_7In_{16}$ and $Tb_6Pt_{12}In_{23}$ were synthesized by an indium flux technique. Arc-melted precursor alloys with the starting compositions $\sim DyPt_3In_6$ and $\sim TbPtIn_4$ were annealed with a slight excess of indium at 1200 K followed by slow cooling (5 K/h) to 870 K. Both indides were investigated by X-ray diffraction on powders and single crystals: *Cmmm*, $a = 1211.1(2)$, $b = 1997.8(3)$, $c = 439.50(6)$ pm, w$R2 = 0.0518$, 1138 F^2 values, 45 variable parameters for $Dy_2Pt_7In_{16}$ and *C*2/*m* $a = 2834.6(4)$, $b = 440.05(7)$, $c = 1477.1(3)$ pm, $\beta = 112.37(1)^\circ$, w$R2 = 0.0753$, 2543 F^2 values, 126 variable parameters for $Tb_6Pt_{12}In_{23}$. The platinum atoms in the terbium compound have a distorted trigonal prismatic coordination. In $Dy_2Pt_7In_{16}$, trigonal and square prismatic coordination occur. The shortest interatomic distances are observed for Pt–In followed by In–In contacts. Considering these strong interactions, both structures can be described by complex three-dimensional $[Pt_7In_{16}]$ and $[Pt_{12}In_{23}]$ networks. The networks leave distorted pentagonal channels in $Dy_2Pt_7In_{16}$, while pentagonal and hexagonal channels occur in $Tb_6Pt_{12}In_{23}$. The crystal chemistry and chemical bonding of the two indides are briefly discussed.

Keywords: Indium compounds; Crystal structure; Indium flux

1. Introduction

Depending on the composition, the rare-earth (*RE*) transition metal (T) indides exhibit largely varying structural motifs. The *RE* metal-rich compounds exhibit typical intermetallic structures which derive from close packed arrangements [1]. Typically, there occur relatively large coordination numbers (CNs). Compounds with a high T content show a tendency for T cluster formation as described recently for several $RE_xT_yIn_z$ indides [2]. In the indium-rich parts of the ternary phase diagrams, compounds with interesting indium substructures exist.

The synthesis techniques for ternary indides strongly depend on the composition of the respective compound. Most of the *RE*- and T-rich indides can easily be prepared by arc-melting of the elements [3]. Crystal growth of such indides is often possible by annealing of the arc-melted buttons in evacuated, sealed, water-cooled quartz ampoules in a high-frequency furnace [4]. If europium or ytterbium are used as *RE* component, arc-melting is no longer possible. Due to the relatively low boiling temperatures, significant evaporation of Eu and Yb occurs leading to unreliable synthesis conditions. Such experimental difficulties can be overcome by reacting the elements in sealed inert metal tubes [3] or by reactions in glassy carbon crucibles in a water-cooled sample chamber of a high-frequency furnace [5].

Indium-rich compounds can also be prepared via arc-melting; however, in many cases only polycrystalline phases form. An excellent method for the growth of single crystals is the reaction in metallic fluxes [6]. The indium flux technique has recently been used for the syntheses of $CeRhIn_5$, $CeIrIn_5$ [7], $Gd_3Pt_4In_{12}$ [8], and $CeNiIn_2$ [9]. We have extended the phase analytical investigations in the indium-rich parts of the *RE*–Pt–In systems. Crystal growths by the indium flux technique

*Corresponding author.
E-mail address: pottgen@uni-muenster.de (R. Pöttgen).

0022-4596/02/$ - see front matter © 2002 Elsevier Science (USA). All rights reserved.
PII: S0022-4596(02)00052-X

revealed the new indides $Tb_6Pt_{12}In_{23}$ and $Dy_2Pt_7In_{16}$, reported herein.

2. Experimental

Starting materials for the synthesis of $Tb_6Pt_{12}In_{23}$ and $Dy_2Pt_7In_{16}$ were ingots of terbium and dysprosium (Johnson–Matthey), platinum powder (Degussa-Hüls, 200 mesh), and indium tear drops (Johnson–Matthey), all with stated purities better than 99.9%). The terbium and dysprosium pieces were first arc-melted to buttons under argon in a miniaturized arc-melting apparatus [3]. The argon was purified before over titanium sponge (900 K), silica gel, and molecular sieves. The pre-melting procedure of the *RE* metals strongly reduces a shattering of these elements during the exothermic reactions. The platinum powder was cold-pressed to small pellets (6 mm diameter). The *RE* metal buttons, the platinum pellets, and pieces of the indium tear drops were then mixed in the 1:1:4 and 1:3:6 atomic ratio and melted to buttons in the arc furnace under an argon pressure of about 600 mbar. The melted ingots were turned over and remelted three times on each side to ensure homogeneity. The total weight losses were always smaller than 0.5%. After the arc-melting procedures we obtained only polycrystalline materials. The silvery products are stable in moist air over a period of several months. No deterioration could be observed. Powders are dark gray.

Single crystals of $Tb_6Pt_{12}In_{23}$ and $Dy_2Pt_7In_{16}$ suitable for X-ray analyses have been grown in an indium flux. The arc-melted $\sim TbPtIn_4$ and $\sim DyPt_3In_6$ buttons were placed in zirconia crucibles together with an excess of 10 wt% indium. The zirconia crucibles were covered with tantalum foil, sealed in evacuated silica tubes and rapidly heated to 1200 K. After 6 h the temperature was lowered by 5 K/h down to 870 K and the tubes were quenched to room temperature by radiative heat loss. The samples could easily be separated from the zirconia crucibles. No reactions with the crucible material were observed. After the slow cooling procedures large light gray crystalline fragments of $Tb_6Pt_{12}In_{23}$ and $Dy_2Pt_7In_{16}$ had formed. The excess indium flux remained at the top of the sample. It could easily be removed with diluted acetic acid. After the correct compositions were evident from the structure refinements, polycrystalline samples of $Tb_6Pt_{12}In_{23}$ and $Dy_2Pt_7In_{16}$ could be obtained via arc-melting. The compositions of the precursor alloys were close to the ideal ones. The slightly different starting compositions were extremely helpful for crystal growth.

Well-shaped single crystals of $Tb_6Pt_{12}In_{23}$ and $Dy_2Pt_7In_{16}$ (Figs. 1 and 2) were analyzed by EDX measurements using a LEICA 420 I scanning electron microscope with TbF_3, DyF_3, elemental platinum, and indium arsenide as standards. No impurity elements were detected. The analyses (15 ± 1 at% Tb: 29 ± 1 at% Pt: 56 ± 1 at% In and 7 ± 1 at% Dy: 30 ± 1 at% Pt: 63 ± 1 at% In) of the single crystals were in good agreement with the ideal compositions of 14.6 at% Tb: 29.2 at% Pt: 56.2 at% In for $Tb_6Pt_{12}In_{23}$ and 8 at% Dy: 28 at% Pt: 64 at% In for $Dy_2Pt_7In_{16}$.

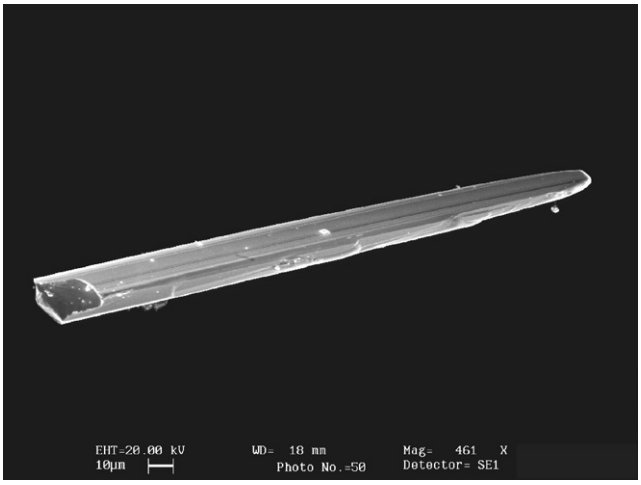

Fig. 1. Scanning electron micrograph of a $Tb_6Pt_{12}In_{23}$ single crystal.

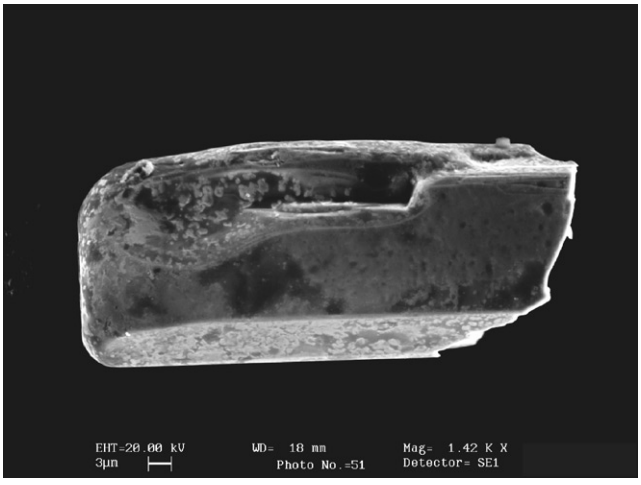

Fig. 2. Scanning electron micrograph of a $Dy_2Pt_7In_{16}$ single crystal.

All samples were characterized through Guinier powder patterns which were recorded with Cu$K\alpha_1$ radiation using α-quartz ($a = 491.30$ pm, $c = 540.46$ pm) as an internal standard. The lattice parameters (see Table 1) were obtained from least-squares fits of the Guinier data. To assure correct indexing, the observed patterns were compared with calculated ones [10] taking the atomic positions from the structure refinements. The lattice parameters obtained from the single crystals were in good accordance with the powder data.

Table 1
Crystal data and structure refinement for $Dy_2Pt_7In_{16}$ and $Tb_6Pt_{12}In_{23}$

Empirical formula	$Dy_2Pt_7In_{16}$	$Tb_6Pt_{12}In_{23}$
Molar mass (g/mol)	3589.67	6024.49
Space group	*Cmmm* (No. 65)	*C*2/*m* (No. 12)
Pearson symbol; Z	*oC*50; 2	*mC*82; 2
Unit-cell dimensions	$a = 1211.1(2)$ pm	$a = 2834.6(4)$ pm
(Guinier powder data)	$b = 1997.8(3)$ pm	$b = 440.05(7)$ pm
	$c = 439.50(6)$ pm	$c = 1477.1(3)$ pm
		$\beta = 112.37(1)^\circ$
	$V = 1.0634\,nm^3$	$V = 1.7038\,nm^3$
Calculated density (g/cm^3)	11.02	11.57
Crystal size (μm^3)	$10 \times 10 \times 80$	$35 \times 40 \times 240$
Transmission ratio (max/min)	2.34	1.76
Absorption coefficient (mm^{-1})	69.7	76.5
F(000)	2924	4906
θ range for data collection	2–33°	2–30°
Range in $h\,k\,l$	$\pm 18, \pm 30, -6 \leqslant l \leqslant 0$	$\pm 30, +6, \pm 20$
Total no. of reflections	4264	5080
Independent reflections	1138 ($R_{int} = 0.0562$)	2543 ($R_{int} = 0.0295$)
Reflections with $I > 2\sigma(I)$	870 ($R_{sigma} = 0.0394$)	2272 ($R_{sigma} = 0.0334$)
Data/restraints/parameters	1138/0/45	2543/0/126
Goodness-of-fit on F^2	1.014	1.177
Final R indices [$I > 2\sigma(I)$]	$R1 = 0.0230$	$R1 = 0.0305$
	$wR2 = 0.0457$	$wR2 = 0.0732$
R indices (all data)	$R1 = 0.0444$	$R1 = 0.0369$
	$wR2 = 0.0518$	$wR2 = 0.0753$
Extinction coefficient	0.00100(2)	0.00030(1)
Largest diff. peak and hole	2.37 and $-2.57\,e/Å^3$	2.83 and $-5.39\,e/Å^3$

Single-crystal intensity data were collected at room temperature by use of a four-circle diffractometer (CAD4) with graphite monochromatized Mo$K\alpha$ (71.073 pm) radiation and a scintillation counter with pulse height discrimination. The scans were taken in the $\omega/2\theta$ mode and empirical absorption corrections were applied on the basis of psi-scan data. All relevant details concerning the data collections are listed in Table 1.

3. Results and discussion

3.1. Structure refinements

Well-shaped single crystals of $Tb_6Pt_{12}In_{23}$ and $Dy_2Pt_7In_{16}$ were isolated from the annealed samples and examined by use of a Buerger camera to establish suitability for intensity data collection. The orthorhombic and monoclinic *C*-centered unit cells of $Tb_6Pt_{12}In_{23}$ and $Dy_2Pt_7In_{16}$ have been determined from 25 carefully centered reflections obtained by an automatic search routine. Examination of the collected data sets showed only the systematic extinctions for a *C*-centering. The space groups with the highest symmetries *Cmmm* ($Dy_2Pt_7In_{16}$) and *C*2/*m* ($Tb_6Pt_{12}In_{23}$) were found to be correct during the structure refinements. Further crystallographic details are listed in Table 1.

The starting atomic parameters were deduced from automatic interpretations of direct methods using SHELXS-97 [11] and both structures were refined using SHELXL-97 [12] (full-matrix least-squares on F^2) with anisotropic displacement parameters for all atoms. The refinements went smoothly to the residuals listed in Table 1. As a check for the correct composition, the occupancy parameters were refined in a separate series of least-squares cycles along with the displacement parameters. All sites were fully occupied within two standard deviations. In the final cycles, the ideal occupancy parameters have been assumed again. Final difference Fourier syntheses were flat (Table 1). The positional parameters and interatomic distances are listed in Tables 2–4. Listings of the observed and calculated structure factors are available.[1]

3.2. Crystal chemistry

Two indium-rich *RE* metal–platinum indides have been synthesized and their crystal structures have been determined from single-crystal diffractometer data. They crystallize with new structure types. Currently, we investigate the *RE* metal platinum indides in more

[1] Details may be obtained from: Fachinformationszentrum Karlsruhe, D-76344 Eggenstein-Leopoldshafen (Germany), by quoting the Registry Nos. CSD-412577 ($Tb_6Pt_{12}In_{23}$) and CSD-412576 ($Dy_2Pt_7In_{16}$).

Table 2
Atomic coordinates and anisotropic displacement parameters (pm^2) for $Dy_2Pt_7In_{16}$ and $Tb_6Pt_{12}In_{23}$

Atom	Wyckoff site	x	y	z	U_{11}	U_{22}	U_{33}	U_{12}/U_{13}[a]	U_{eq}
$Dy_2Pt_7In_{16}$ (space group Cmmm)									
Dy1	4*h*	0.82979(6)	0	$\frac{1}{2}$	78(3)	68(3)	73(3)	0	73(2)
Pt1	2*c*	$\frac{1}{2}$	0	$\frac{1}{2}$	91(4)	80(3)	58(4)	0	76(2)
Pt2	4*j*	0	0.27558(3)	$\frac{1}{2}$	57(2)	58(2)	57(3)	0	57(1)
Pt3	8*p*	0.27619(3)	0.39055(2)	0	65(2)	123(2)	60(2)	−6(1)	83(1)
In1	4*g*	0.63185(9)	0	0	86(5)	105(4)	48(5)	0	80(2)
In2	8*q*	0.13008(6)	0.38679(4)	$\frac{1}{2}$	69(3)	70(3)	82(4)	−10(2)	73(2)
In3	8*p*	0.13473(6)	0.27644(4)	0	89(4)	144(4)	53(4)	−15(3)	95(2)
In4	8*q*	0.12466(7)	0.16317(4)	$\frac{1}{2}$	110(4)	89(3)	93(4)	48(3)	97(2)
In5	4*i*	0	0.92644(5)	0	56(4)	82(4)	120(5)	0	86(2)
$Tb_6Pt_{12}In_{23}$ (space group C2/m)									
Tb1	4*i*	0.45413(3)	0	0.30114(5)	77(4)	49(3)	62(3)	41(3)	58(2)
Tb2	4*i*	0.82171(3)	0	0.92201(5)	85(4)	48(3)	61(3)	41(3)	61(2)
Tb3	4*i*	0.83410(3)	0	0.46938(5)	63(3)	59(3)	65(3)	30(2)	61(2)
Pt1	4*i*	0.25299(2)	0	0.36389(4)	55(3)	32(3)	45(2)	21(2)	44(1)
Pt2	4*i*	0.38127(2)	0	0.85045(4)	49(3)	55(3)	45(2)	22(2)	49(1)
Pt3	4*i*	0.32069(2)	0	0.08940(4)	63(3)	32(3)	64(2)	27(2)	52(1)
Pt4	4*i*	0.90070(2)	0	0.36563(4)	66(3)	63(3)	43(2)	27(2)	56(1)
Pt5	4*i*	0.96746(2)	0	0.14225(4)	73(3)	42(3)	79(3)	3(2)	72(1)
Pt6	4*i*	0.39081(2)	0	0.64133(4)	58(3)	50(3)	51(2)	21(2)	53(1)
In1	4*i*	0.40793(4)	0	0.04986(7)	52(5)	41(5)	40(4)	16(3)	45(2)
In2	4*i*	0.71338(4)	0	0.43450(7)	57(5)	44(5)	27(4)	19(3)	42(2)
In3	2*c*	0	0	$\frac{1}{2}$	26(7)	60(7)	70(6)	8(5)	55(3)
In4	4*i*	0.76219(4)	0	0.08351(7)	54(5)	47(5)	53(4)	33(4)	48(2)
In5	4*i*	0.14577(4)	0	0.27948(7)	58(5)	50(5)	43(4)	21(4)	50(2)
In6	4*i*	0.04543(4)	0	0.33334(7)	64(5)	38(5)	66(4)	11(4)	60(2)
In7	4*i*	0.94389(4)	0	0.93853(7)	70(5)	49(5)	56(4)	23(4)	59(2)
In8	4*i*	0.32641(4)	0	0.28166(7)	83(5)	87(5)	56(4)	44(4)	70(2)
In9	4*i*	0.87649(4)	0	0.17059(7)	76(5)	56(5)	45(4)	9(4)	63(2)
In10	4*i*	0.47123(4)	0	0.82555(7)	49(5)	52(5)	63(4)	29(4)	53(2)
In11	4*i*	0.42464(4)	0	0.49405(7)	136(6)	61(5)	60(4)	53(4)	81(2)
In12	4*i*	0.72732(4)	0	0.24450(7)	81(5)	40(5)	35(4)	25(4)	51(2)

[a] $U_{23} = U_{13} = 0$ for $Dy_2Pt_7In_{16}$ and $U_{12} = U_{23} = 0$ for $Tb_6Pt_{12}In_{23}$.
Note: U_{eq} is defined as one-third of the trace of the orthogonalized U_{ij} tensor. The anisotropic displacement factor exponent takes the form: $-2\pi^2[(ha^*)^2U_{11}+\cdots+2hka^*b^*U_{12}]$.

Table 3
Interatomic distances (pm), calculated with the lattice parameters taken from X-ray powder data of $Dy_2Pt_7In_{16}$

Dy:	4	Pt3	316.7(1)	Pt3:	2	In4	272.4(1)	In3:	2	Pt2	273.7(1)
	2	In1	325.2(1)		1	In1	280.0(1)		1	Pt3	285.2(1)
	2	In4	330.6(1)		1	In5	280.4(1)		1	In3	298.5(2)
	2	In2	331.1(1)		2	In2	282.2(1)		2	In2	311.3(1)
	4	In5	335.2(1)		1	In3	285.2(1)		2	In4	315.7(1)
	1	Pt1	399.4(1)		2	Dy	316.7(1)		1	In3	326.4(2)
	1	Dy	412.3(2)		1	In3	350.6(1)	In4:	1	Pt2	270.6(1)
	2	Dy	439.5(1)	In1:	2	Pt1	271.6(1)		2	Pt3	272.4(1)
Pt1:	4	In1	271.6(1)		2	Pt3	280.0(1)		1	In4	302.0(2)
	4	In2	275.6(1)		4	In2	315.4(1)		1	In2	313.4(1)
	2	Dy	399.4(1)		1	In1	319.4(2)		2	In3	315.7(1)
Pt2:	2	In4	270.6(1)		2	Dy	325.2(1)		2	In5	321.2(1)
	2	In2	272.4(1)	In2:	1	Pt2	272.4(1)		1	Dy	330.6(1)
	4	In3	273.7(1)		1	Pt1	275.6(1)	In5:	2	Pt3	280.4(1)
					2	Pt3	282.2(1)		1	In5	293.9(2)
					2	In3	311.3(1)		4	In4	321.2(1)
					1	In4	313.4(1)		4	Dy	335.2(1)
					1	In2	315.1(2)				
					2	In1	315.4(1)				
					1	Dy	331.1(1)				

Note: All distances within the first coordination sphere are listed. Standard deviations are given in parentheses.

Table 4
Interatomic distances (pm), calculated with the lattice parameters taken from X-ray powder data of $Tb_6Pt_{12}In_{23}$

Tb1:	2	Pt4	302.3(1)	Tb3:	1	Pt4	284.9(1)	Pt3:	2	In9	270.9(1)	In1:	1	Pt2	274.8(1)	In5:	1	Pt1	281.2(1)	In9:	1	Pt4	269.6(1)
	2	In9	319.0(1)		2	Pt1	313.5(1)		1	In4	273.4(1)		1	Pt3	274.9(1)		2	Pt2	282.7(1)		2	Pt3	270.9(1)
	1	In11	326.1(1)		2	In2	318.2(1)		2	In4	273.7(1)		2	Pt5	279.2(1)		2	Pt6	286.5(1)		1	Pt5	276.5(1)
	2	In6	329.1(1)		1	In2	326.1(1)		1	In1	274.9(1)		2	In7	314.0(1)		2	In2	322.8(1)		1	In4	299.7(2)
	1	In10	331.6(1)		2	Pt6	328.1(1)		1	In8	278.2(1)		2	In9	316.6(1)		1	In6	323.2(2)		2	In1	316.6(1)
	2	Pt5	334.2(1)		2	In11	329.4(1)		2	Tb2	331.8(1)		1	In10	321.3(2)		1	In7	325.6(2)		2	Tb1	318.9(1)
	1	In1	343.4(1)		2	In8	348.1(1)		1	Tb1	388.4(1)		2	Tb2	329.7(1)		2	In12	337.1(1)		2	In8	336.5(1)
	2	In3	350.0(1)		1	In5	353.2(1)		1	Tb2	397.6(1)		1	Tb1	343.4(1)		1	Tb2	343.5(1)		1	Tb2	339.9(1)
	1	In8	352.1(1)		1	In12	354.2(1)	Pt4:	1	In9	269.6(1)	In2:	1	Pt6	273.1(1)		1	Tb3	353.2(1)	In10:	1	Pt2	271.1(1)
	1	In11	361.2(1)		1	In6	354.7(1)		1	In3	278.9(1)		1	Pt1	276.0(1)		2	In10	378.6(1)		2	Pt5	273.1(1)
	1	Pt3	388.4(1)		1	Pt1	409.7(1)		2	In11	281.4(1)		2	Pt1	284.3(1)	In6:	2	Pt6	278.1(1)		1	Pt6	280.7(1)
	1	Pt6	414.7(1)		2	Tb3	440.1(1)		1	Tb3	284.9(1)		1	In12	297.9(1)		1	Pt5	284.7(1)		2	In7	303.5(1)
	2	Tb1	440.1(1)	Pt1:	2	In12	273.9(1)		2	In8	297.1(1)		2	In2	313.7(1)		2	In10	311.9(1)		2	In6	311.9(1)
Tb2:	2	Pt2	318.9(1)		1	In2	276.0(1)		2	Tb1	302.3(1)		2	Tb3	318.2(1)		1	In3	318.3(1)		1	In1	321.3(2)
	2	In12	319.7(1)		1	In8	278.0(1)	Pt5:	2	In10	273.1(1)		2	In5	322.8(1)		2	In11	322.7(1)		1	Tb1	331.6(1)
	2	In4	321.8(1)		1	In5	281.2(1)		1	In9	276.5(1)		1	Tb3	326.1(1)		1	In5	323.2(2)		2	In5	378.6(1)
	2	In1	329.7(1)		2	In2	284.3(1)		2	In1	279.2(1)	In3:	2	Pt4	275.9(1)		2	Tb1	329.1(1)	In11:	1	Pt6	269.1(1)
	2	Pt3	331.8(1)		2	Tb3	313.5(1)		1	In7	282.3(1)		4	In11	304.4(1)		1	Tb3	354.6(1)		2	Pt4	281.4(1)
	1	In7	337.8(1)		1	Tb2	393.9(1)		1	In6	284.7(1)		2	In6	318.3(1)	In7:	2	Pt2	281.5(1)		2	In3	304.5(1)
	1	In9	339.9(1)		1	Tb3	409.7(1)		1	In7	316.6(1)		4	Tb1	350.0(1)		1	Pt5	282.3(1)		2	In6	322.7(1)
	1	In4	340.6(1)	Pt2:	1	In10	271.1(1)		2	Tb1	334.2(1)	In4:	1	Pt3	273.4(1)		1	In7	300.3(2)		1	Tb1	326.1(1)
	1	In5	343.5(1)		1	In1	274.8(1)		1	Tb2	417.4(1)		2	Pt3	273.7(1)		2	In10	303.5(1)		2	Tb3	329.4(1)
	1	Pt1	393.9(1)		2	In7	281.5(1)	Pt6:	1	In11	269.1(1)		1	In12	290.2(2)		2	In1	314.0(1)		1	In8	330.9(2)
	1	Pt3	397.6(1)		2	In5	282.7(1)		1	In2	273.1(1)		1	In9	299.7(2)		1	Pt5	316.6(1)		1	Tb1	361.2(1)
	1	In8	413.1(2)		1	In12	285.6(1)		2	In6	278.1(1)		2	In4	317.9(2)		1	In5	325.6(2)	In12:	2	Pt1	273.9(1)
	1	Pt5	417.4(1)		2	Tb2	318.9(1)		1	In10	280.7(1)		2	Tb2	321.8(1)		1	Tb2	337.8(1)		1	Pt2	285.6(1)
	2	Tb2	440.1(1)		1	Pt6	320.2(1)		2	In5	286.5(1)		1	Tb2	340.6(1)	In8:	1	Pt1	278.0(1)		1	In4	290.2(2)
									1	Pt2	320.2(1)		2	In8	355.9(1)		1	Pt3	278.2(1)		1	In2	297.9(2)
									2	Tb3	328.1(1)						2	Pt4	297.1(1)		2	Tb2	319.7(1)
									1	Tb1	414.7(1)						1	In11	330.9(2)		2	In5	337.1(1)
																	2	In9	336.5(1)		2	In8	344.4(1)
																	2	In12	344.4(1)		1	Tb3	354.2(1)
																	2	Tb3	348.1(1)				
																	1	Tb1	352.1(1)				
																	2	In4	355.9(1)				

Note: All distances within the first coordination sphere are listed. Standard deviations are given in parentheses.

detail. So far, $Tb_6Pt_{12}In_{23}$ and $Dy_2Pt_7In_{16}$ are unique examples for these peculiar structure types. Attempts to study *RE* substitution resulted in new compounds with different compositions. The complex phase relationships in the *RE* metal platinum indium systems are not yet completely established.

Projections of the $Tb_6Pt_{12}In_{23}$ and $Dy_2Pt_7In_{16}$ structures are presented in Fig. 3. A common geometrical motif of both structures are platinum-centered trigonal prisms formed by two *RE* and four indium atoms. These trigonal prisms are condensed via common edges formed by the *RE* metal atoms, by Tb–In, or by In–In bonds. This type of trigonal prism occurs in various indium-rich indides, e.g., $GdRhIn_2$ [13] or $CeNiIn_4$ [14]. In addition to the trigonal prismatic platinum coordination, the $Dy_2Pt_7In_{16}$ structure has also a square prismatic platinum coordination.

The shortest interatomic distances in both structures occur for the Pt–In contacts. The platinum atoms have six, seven, or eight nearest indium neighbors at Pt–In distances ranging from 271 to 285 pm in $Dy_2Pt_7In_{16}$, and from 269 to 317 pm in $Tb_6Pt_{12}In_{23}$. The shorter of these Pt–In distances are even below the sum of the covalent radii [15] of 279 pm. We can thus assume a significant degree of Pt–In bonding in the structures of $Tb_6Pt_{12}In_{23}$ and $Dy_2Pt_7In_{16}$. Similar Pt–In distances have recently been observed in a variety of alkaline earth (AE) metal–platinum–indides. A summary of the various platinum–indium coordinations is given in Ref. [16]. The $PtIn_7$ units are observed in $Tb_6Pt_{12}In_{23}$ for the first time. The longer Pt5–In7 contact at 317 pm in $Tb_6Pt_{12}In_{23}$ may only be considered as very weakly bonding; however, the In7 atoms certainly belong to the coordination shell of Pt5.

An interesting structural feature are the condensed distorted square $PtIn_8$ prisms in the $Dy_2Pt_7In_{16}$ structure. As emphasized in Fig. 4, these $PtIn_8$ prisms are condensed via common rectangular faces forming a one-dimensional infinite strand along the *c* direction. So far, square prisms have only been observed in binary $PtIn_2$ [17] with fluorite structure.

Due to the high indium content of both indides (56.2 at% for $Tb_6Pt_{12}In_{23}$ and 64 at% for $Dy_2Pt_7In_{16}$)

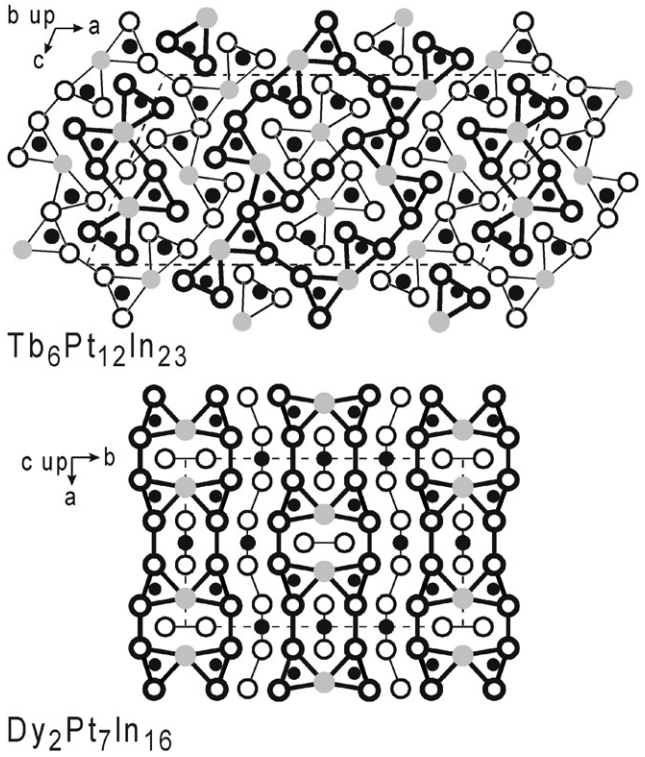

Fig. 3. Projections of the $Dy_2Pt_7In_{16}$ and $Tb_6Pt_{12}In_{23}$ structures along the short axis. The dysprosium (terbium), platinum, and indium atoms are drawn as gray, black filled, and black open circles, respectively. The trigonal prisms around the platinum atoms are emphasized. All atoms lie on mirror planes at $z = 0$ (thin lines) and $z = 1/2$ (thick lines) for $Dy_2Pt_7In_{16}$ and at $y = 0$ (thin lines) and $y = 1/2$ (thick lines) for $Tb_6Pt_{12}In_{23}$.

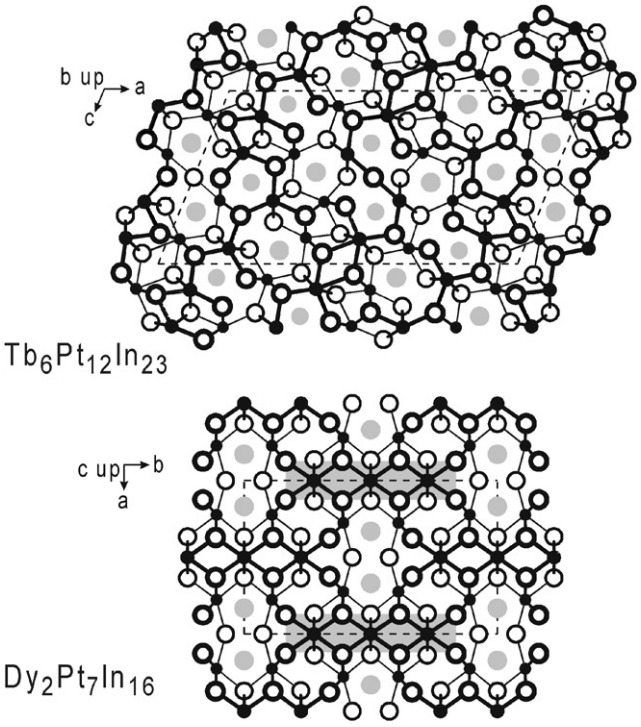

Fig. 4. View of the $Dy_2Pt_7In_{16}$ and $Tb_6Pt_{12}In_{23}$ structures along the short unit cell axes. The three-dimensional $[Pt_7In_{16}]$ and $[Pt_{12}In_{23}]$ networks are emphasized. For clarity, only the Pt–In bonds are drawn. Dysprosium (terbium), platinum, and indium atoms are drawn as gray, filled, and open circles, respectively. The shaded areas in the $Dy_2Pt_7In_{16}$ structure emphasize the square prismatic platinum coordination.

we observe a variety of In–In contacts. The In–In distances range from 294 to 326 pm in $Dy_2Pt_7In_{16}$ and from 290 to 379 pm in $Tb_6Pt_{12}In_{23}$. Most of these In–In distances are shorter than in the tetragonal body-centered structure of elemental indium ($a = 325.2$ pm, $c = 494.7$ pm) [18], where each indium atom has four nearest neighbors at 325 pm and eight further neighbors at 338 pm. The average In–In distance for the twelve neighbors amounts to 333 pm. Thus, most In–In contacts in $Dy_2Pt_7In_{16}$ and $Tb_6Pt_{12}In_{23}$ can be considered as significantly bonding. A much weaker bonding character should be ascribed to the In4–In8 (356 pm) and In5–In10 (379 pm) contacts. Again, the In8 and In10 atoms still belong to the coordination shells of In4 and In5, respectively.

The indium atoms have between five and eight nearest indium neighbors. The CN can be lower than that in elemental indium (CN 12), since in the ternary compounds the indium atoms have also *RE* and platinum neighbors. Nevertheless, parts of the indium substructures of $Dy_2Pt_7In_{16}$ and $Tb_6Pt_{12}In_{23}$ resemble the indium structure. In two previous papers we already emphasized, that structures of indium-rich intermetallics contain distorted indium centered indium cubes as structural motifs [13,19]. In the two structures presented here and in the structure of $Yb_2Pd_6In_{13}$ [20] fragments of these cubes remain. A more detailed analyses of these indium substructures will be published in a forthcoming paper [20].

While the shortest Pt–Pt distance in $Dy_2Pt_7In_{16}$ is at 437 pm, there might be some weak Pt2–Pt6 bonding in the structure of $Tb_6Pt_{12}In_{23}$. This Pt2–Pt6 distance of 320 pm, however, is larger than the Pt–Pt distance of 277 pm in *fcc* platinum [18].

Considering the strong Pt–In and In–In bonding in both structure types, one can best describe the structures by polyanions. In view of the trend of the electronegativities (Dy: 1.22, Pt: 2.28, In: 1.78 on the Pauling scale) we can assume a charge transfer from the more electropositive dysprosium to the more electronegative platinum and indium atoms. The same holds true for the terbium compound. In emphasizing the covalently bonded polyanions, both formulae can to a first approximation be written as $(Tb^{3+})_6\,[Pt_{12}In_{23}]^{18-}$ and $(Dy^{3+})_2[Pt_7In_{16}]^{6-}$. The polyanionic networks are presented in Fig. 4. For clarity only the Pt–In contacts are drawn. The networks leave distorted pentagonal channels in $Dy_2Pt_7In_{16}$, while pentagonal and hexagonal

channels occur in $Tb_6Pt_{12}In_{23}$. Polyanions with one-dimensional (1D) channels often occur in this kind of indium intermetallics. Further examples are the structures of $PrNiIn_2$ [21], $Nd_5Ni_6In_{11}$ [22], or $SmRhIn_2$ [23].

The RE metal atoms are located within the 1D channels of the $[Pt_7In_{16}]$ and $[Pt_{12}In_{23}]$ matrices. They are well separated from each other. The shortest Dy–Dy and Tb–Tb distances are at 412 and 440 pm, respectively. The CNs of the *RE* metal atoms range from 18 to 20. This is usually observed for such intermetallics. Bonding of the *RE* atoms to the polyanionic network is governed by *RE*−Pt contacts. In both structures, the *RE* atoms have at least one platinum atom as nearest neighbor. The strongest bonding occurs for the Tb3 atoms of $Tb_6Pt_{12}In_{23}$, where the Tb4–Pt4 distance of 285 pm is even shorter than the sum of the covalent radii of 288 pm [15].

Acknowledgments

We are grateful to J. Göcke for the EDX analyses and to the Degussa-Hüls AG for a generous gift of platinum powder. This work was financially supported by the Fonds der Chemischen Industrie and the Deutsche Forschungsgemeinschaft. V.I.Z. is indebted to the Alexander von Humboldt Foundation for a research stipend.

References

[1] Ya.M. Kalychak, J. Alloys Compounds 262–263 (1997) 341.
[2] Ya.M. Kalychak, V.I. Zaremba, Ya.V. Galadzhun, Kh.Yu. Miliyanchuk, R.-D. Hoffmann, R. Pöttgen, Chem. Eur. J. 7 (2001) 5343.
[3] R. Pöttgen, Th. Gulden, A. Simon, GIT Fachz. Lab. 43 (1999) 133.
[4] D. Niepmann, Yu.M. Prots', R. Pöttgen, W. Jeitschko, J. Solid State Chem. 154 (2000) 329.
[5] D. Kußmann, R.-D. Hoffmann, R. Pöttgen, Z. Anorg. Allg. Chem. 624 (1998) 1727.
[6] P.C. Canfield, Z. Fisk, Philos. Mag. B 65 (1992) 1117.
[7] E.G. Moshopoulou, Z. Fisk, J.L. Sarrao, J.D. Thompson, J. Solid State Chem. 158 (2001) 25.
[8] U.Ch. Rodewald, V.I. Zaremba, Ya.V. Galadzhun, R.-D. Hoffmann, R. Pöttgen, Z. Anorg. Allg. Chem. 628 (2002) 2293.
[9] V.I. Zaremba, Ya.M. Kalychak, Yu.B. Tyvanchuk, R.-D. Hoffmann, M.H. Möttgen, Z. Naturforsch. 57b (2002) 791.
[10] K. Yvon, W. Jeitschko, E. Parthé, J. Appl. Crystallogr. 10 (1977) 73.
[11] G.M. Sheldrick, Shelxs-97, Program for the Solution of Crystal Structures, University of Göttingen, 1997.
[12] G.M. Sheldrick, Shelxl-97, Program for Crystal Structure Refinement, University of Göttingen, 1997.
[13] R.-D. Hoffmann, R. Pöttgen, V.I. Zaremba, Ya.M. Kalychak, Z. Naturforsch. 55b (2000) 834.
[14] R. Pöttgen, J. Mater. Chem. 5 (1995) 769.
[15] J. Emsley, The Elements, Clarendon Press, Oxford, 1989.
[16] Ya.V. Galadzhun, V.I. Zaremba, H. Piotrowski, P. Mayer, R.-D. Hoffmann, R. Pöttgen, Z. Naturforsch. 55b (2000) 1025.
[17] E. Zintl, A. Harder, W. Haucke, Z. Phys. Chem. B 35 (1937) 354.
[18] J. Donohue, The Structures of the Elements, Wiley, New York, 1974.
[19] R.-D. Hoffmann, R. Pöttgen, Chem. Eur. J. 6 (2000) 600.
[20] V.I. Zaremba, V.P. Dubenskiy, Ya.M. Kalychak, R.-D. Hoffmann, R. Pöttgen, Solid State Sciences, in press.
[21] V.I. Zaremba, Ya.M. Kalychak, V.P. Dubenskiy, R.-D. Hoffmann, R. Pöttgen, J. Solid State Chem. 152 (2000) 560.
[22] R. Pöttgen, R.-D. Hoffmann, R.K. Kremer, W. Schnelle, J. Solid State Chem. 142 (1999) 180.
[23] V.I. Zaremba, V.P. Dubenskiy, R. Pöttgen, Z. Naturforsch. 57b (2002) 798.